Molecular Weight Dependence of Chain Orientation and Optical Constants of Thin Films of the Conjugated Polymer MEH-PPV

Kaloian Koynov,*,† Ayi Bahtiar,†,§ Taek Ahn,⊥,† Rodrigo M. Cordeiro,† Hans-Heinrich Hörhold,‡ and Christoph Bubeck†

Max Planck Institute for Polymer Research, Ackermannweg 10, D-55128 Mainz, Germany, and Institute for Organic Chemistry and Macromolecular Chemistry, University of Jena, Humboldtstr. 10, 07743 Jena, Germany

Received May 18, 2006; Revised Manuscript Received September 5, 2006

ABSTRACT: We have studied thin films of the conjugated polymer poly[2-methoxy-5-(2′-ethylhexyloxy)-1,4-phenylenevinylene] (MEH-PPV), prepared from polymer samples whose weight-average molecular weight (M_w) was varied in the broad range of 10−1600 kg/mol. Anisotropic refractive index measurements by means of waveguide prism coupling and reflectometry as well as polarized infrared spectroscopy were used to analyze the polymer chain orientation in the films. We found that the film morphology depends significantly on the molecular weight, especially in the range M_w < 400 kg/mol. Thin films of high molecular weight MEH-PPV have most polymer chain segments oriented parallel to the film plane—in contrast to low molecular weight samples which have nearly random orientation of the chain segments. Appropriate choice of molecular weight enables fine-tuning of the refractive index of slab waveguides and reduction of their mode propagation losses to less than 1 dB/cm.

Introduction

Derivatives of poly(*p*-phenylenevinylene) (PPV) are intensively studied because of their outstanding semiconducting, luminescent, and nonlinear optical properties.[1−8] In particular, poly[2-methoxy-5-(2′-ethylhexyloxy)-1,4-phenylenevinylene] (MEH−PPV, see Scheme 1 for its chemical structure) is frequently used as model material to gain basic understanding of the photophysics of a typical conjugated polymer.[1−4] It is soluble in common organic solvents and can be easily processed to thin films by spin-coating. It has been shown that such films exhibit uniaxial anisotropy due to preferred alignment of the polymer chains in the plane of the film.[9−15] Because the main electric polarizability and the transition dipole moment of the conjugated π-electron system are parallel to the chain direction of a conjugated polymer, the anisotropic orientation of chain segments is strongly correlated with significant birefringence of the films; i.e., the refractive indices at transverse electric (TE) and transverse magnetic (TM) polarizations differ considerably with $n_{TE} > n_{TM}$.[9−17] It is remarkable, however, that reports of basic optical properties of thin films of MEH-PPV such as their refractive index and absorption coefficient show significant disagreements.[6,10−13] This discrepancy of the published data is not limited to films of MEH-PPV only but is observed also for many other conjugated polymers.[18] There are two main reasons for inconsistencies in the reports of optical constants of thin polymer films: (i) Although a broad variety of techniques is currently used for the measurement of the refractive index and its anisotropy, their precise determination (especially of n_{TM}) in very thin films is still a major challenge.[18] (ii) The morphology of thin polymer films, and consequently the values of n_{TE} and n_{TM}, can depend significantly on the molecular weight,[16,19−21] the film thickness,[19,22] and the preparation conditions of the films.[4,23]

Scheme 1. Chemical Structure of Poly[2-methoxy-5-(2′-ethylhexyloxy)-1,4-phenylenevinylene] (MEH-PPV)

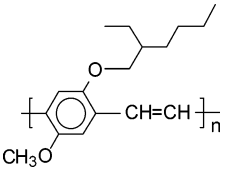

It was reported recently that the molecular weight in particular has strong impact on morphology and optoelectronic properties of thin films of conjugated polymers. This is observed not only in the case of MEH-PPV[14,15,24] but also in polydiacetylene,[20] polythiophenes,[25−28] and polyfluorenes,[29−32] for example.

The aim of this work is to present a comprehensive study on the influence of the molecular weight on the polymer chain orientation in thin spin-coated films of MEH-PPV by means of transmission and reflection spectroscopy, prism coupling of slab waveguides, and FTIR spectroscopy. We will show that higher molecular weight MEH-PPVs have an increased amount of polymer chain segments aligned parallel to the film plane as compared to low molecular weight samples. As a consequence, important optical constants of the films such as refractive index, absorption coefficient, and waveguide propagation loss coefficient depend significantly on the molecular weight of the polymer.

Experimental Section

It is necessary to apply different synthetic routes to obtain MEH-PPVs with a large variation of molecular weight. The frequently used, so-called Gilch dehydrohalogenation route[33,34] yields polymers which have a weight-average molecular weight M_w on the order of 10^2-10^3 kg/mol. However, M_w can be significantly reduced by appropriate choice of end-cappers in the synthetic process. Another synthetic approach to MEH-PPV with very well-defined chain structure was realized by using the Horner-type polycondensation

† Max Planck Institute for Polymer Research.
‡ University of Jena.
§ Present address: Department of Physics, University of Padjadjaran Bandung, Jl. Jatinangor km. 21 Sumedang, 45363, Indonesia.
⊥ Present address: Korea Research Institute of Chemical Technology, P.O. Box 107, Yuseong, Daejeon 305-600, Korea.
* Corresponding author. E-mail: koynov@mpip-mainz.mpg.de.

10.1021/ma0611164 CCC: $33.50
Published on Web 11/10/2006

Table 1. Properties of MEH-PPVs from Different Synthesis Pathways and Molecular Weights[a]

polymer	route	M_w [kg/mol]	M_n [kg/mol]	M_w/M_n	λ_{max} [nm]	α_{max} [10^4 cm^{-1}]	$\alpha_{gw}(TE_0)$ [dB/cm]	$\alpha_{gw}(TM_0)$ [dB/cm]
1	Gilch	9.3	4.8	1.94	472	13.2	0.5 ± 0.3	0.7 ± 0.3
2	Horner	13	6.4	2.03	474	13.9	0.9 ± 0.4	0.6 ± 0.3
3[b]	Horner	25	9.1	2.75	477	15.0	0.5 ± 0.3	
4	Horner	40.3	14.1	2.86	489	16.6	0.5 ± 0.3	0.5 ± 0.3
5	Gilch	128	24.6	5.20	494	14.6	5.1 ± 0.4	0.5 ± 0.3
6	Gilch	265	87.1	3.04	489	18.2	6.2 ± 1.6	0.5 ± 0.3
7	Gilch	276	105	2.63	491	18.4	6.4 ± 1.6	1.0 ± 0.3
8	Gilch	420	108	3.89	495	19.1	30 ± 5	0.6 ± 0.3
9	Gilch	1600	130	12.3	495	19.4		

[a] M_w = weight-average molecular weight, M_n = number-average molecular weight. All optical data are from studies of thin films: λ_{max} = wavelength of absorption maximum, α_{max} = intrinsic absorption coefficient at λ_{max}, α_{gw} = attenuation loss of guided waves of TE_0 and TM_0 modes, measured at 1064 nm. [b] Data are from ref 6.

route which yields polymers with M_w in the typical order of several 10 kg/mol.[23,35]

We have investigated nine different MEH-PPV samples **1**−**9** (listed in Table 1) with M_w in the range of 10−1600 kg/mol. The MEH-PPVs **2**−**4** were synthesized via the polycondensation route using the Horner carbonylolefination as the step growth polymerization process.[35] The synthesis of **7** was performed via Gilch dehydrohalogenation as described recently.[36] MEH-PPVs **1**, **5**, **6**, **8**, and **9** were also synthesized via the Gilch route. **1**, **6**, and **8** were obtained from American Dye Source (ADS), Canada, and **9** was provided by Covion GmbH, Germany. Molecular weights were measured by gel permeation chromatography (GPC) using polystyrene standards and THF as eluent. All MEH-PPV solutions were filtered (0.5 or 1 μm syringe filters) prior to the GPC measurements.

Thin films were prepared by spin-coating from freshly prepared and filtered (0.5 or 1 μm syringe filters) toluene solutions at ambient atmosphere under a laminar flow hood to minimize dust particles as descibed in detail recently.[6] We used freshly cleaned fused silica substrates for the UV/vis/NIR range and silicon wafers and freshly evaporated gold layers on glass for the IR range with typical substrate sizes of $25 \times 35 \times 1$ mm^3. We varied the concentration by weight (1−7%) and spinning speed (500−9000 rpm at quick acceleration) to control the film thickness. While the low-M_w MEH-PPVs **1**−**4** were easily dissolved in concentrations by weight up to 7%, we did not use the higher molecular weight polymers **5**−**9** in such high concentrations because their solutions have very large viscosities. Gelation problems appeared in the case of polymer **9** at concentrations >1 wt %, and that is why we were not able to spin-coat films thicker than 150 nm from this polymer.

The films were placed subsequently in a vacuum oven at elevated temperatures ($T \approx 50$ °C) for about 6 h to remove residual solvent. The thickness d and the average surface roughness of the films were measured with a Tencor model P10 profilometer. In order to increase the precision, we have measured the film thickness for each film at several step profiles (typically 8) in the region where the optical experiments were performed and used the average value of these measurements. We have used films with thickness $d \approx$ 50−70 nm for spectroscopic studies and thicker films (400−800 nm) for optical waveguides.

We have applied the so-called doctor-blading technique[37] to prepare films with d up to 10 μm from polymer **7** by means of the Erichsen model Coatmaster 509/MC-1 film drawing system in the following way: The film preparation frame was filled with a highly concentrated polymer solution and pulled along the surface of a fused silica substrate. Films prepared this way, however, showed some thickness variations. Therefore, their thickness was evaluated only by the prism coupling method described below.

Transmission and reflection spectra of thin films ($d \approx 50-70$ nm) on fused silica substrates were measured with a spectrophotometer (Perkin-Elmer model Lambda 900). Intrinsic absorption coefficients α were evaluated from transmission spectra after correction of reflection losses at film/air and film/substrate interfaces as described in earlier works.[6,38] These corrections usually cause blue shifts of λ_{max} relative to the uncorrected spectra.[6] The spectra of $n_{TE}(\lambda)$ of the films were obtained by reflectometry at nearly perpendicular incidence and were evaluated by means of Fresnel's equations.[6,38]

The refractive indices of MEH-PPV waveguides (with thickness in the range of 400 nm−10 μm) for both TE and TM polarization were determined by prism coupling using the m-line technique[39] as described earlier.[7] The following lasers were used: HeNe (633 nm) and an optical parametric generator which can be tuned in the range of 680−2000 nm (EKSPLA model PG 501 pumped by the second harmonic of a ps-Nd:YAG laser, EKSPLA model PL 2143B). We were able to excite both TE_0 and TE_1 (respectively TM_0 and TM_1) at the appropriate laser wavelength and used these two modes to calculate the refractive index and film thickness simultaneously. The obtained values of film thicknesses were in good agreement with those measured with the step profiler.

Waveguide loss experiments were performed by use of the CW Nd:YAG (1064 nm) laser and the setup described earlier.[40] The scattered light from the waveguide was imaged by a lens onto a diode array. Attenuation loss coefficients α_{gw} were determined from the scattered light intensity as a function of distance from the coupling prism. The detection limit of this method is on the order of $\alpha_{gw} \approx 0.5$ dB/cm.

Infrared spectra were recorded with a Nicolet model Magna 850 FTIR spectrometer at two configurations: Transmission spectra of thin films ($d \approx 70$ nm) deposited on silicon wafers were measured at normal incidence. Reflection spectra using p-polarized light at grazing incidence were measured with MEH-PPV films ($d \approx 70$ nm) that were spin-cast on top of 50 nm thick gold layers prepared before by thermal evaporation onto glass slides. This kind of infrared reflection−absorption spectroscopy (IRRAS) on metal surfaces provides improved detection sensitivity and a well-defined polarization state with the electric field vector **E** perpendicular to the film plane.[41] The comparison of IRRAS with transmission at normal incidence where **E** is parallel to the film plane enables orientation studies as reviewed earlier.[42] As all films were prepared and studied at ambient air we have also used FTIR spectroscopy to verify that our results were not influenced by photooxidation of the MEH-PPV films.

Results and Discussion

Refractive Index and Absorption Coefficient. The dispersions of the refractive index $n(\lambda)$ and the intrinsic absorption coefficient $\alpha(\lambda)$ of thin ($d \approx 50-70$ nm) MEH-PPV films were determined by quantitative evaluation of transmission and reflection spectra of thin films on fused silica substrates similar to earlier work.[6,38] In these measurements polarized light with electric field vector **E** parallel to the film plane was used. Figure 1 shows selected spectra $\alpha(\lambda)$ of polymers **1**, **3**, **4**, **6**, **8**, and **9**. The absorption coefficients α_{max} and wavelengths λ_{max} of the maximum of the main absorption band are shown in Table 1 for all investigated polymers. The data of λ_{max} have an estimated uncertainty of ± 2 nm because of broad absorption bands. The experimental error of α_{max} is on the order of 5% and is caused

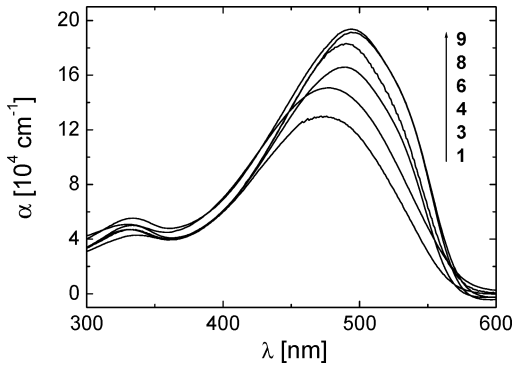

Figure 1. Spectra of the intrinsic absorption coefficient α of thin films of MEH-PPVs with different molecular weight. The spectra correspond to MEH-PPVs **1**, **3**, **4**, **6**, **8**, and **9** (see Table 1).

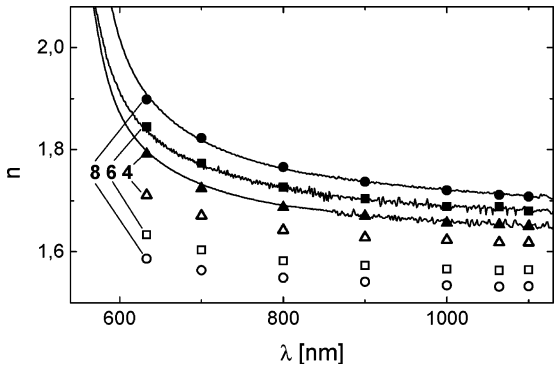

Figure 2. Dispersions of refractive indices of MEH-PPVs **4**, **6**, and **8**. Data points are from prism coupling experiments with optical waveguides at TE polarization (full symbols) and TM polarization (open symbols). Lines are from transmission−reflection experiments at TE polarization.

mainly by the experimental error of *d*. The films of **1**−**4** and **6**−**9** show a systematic trend to larger values of α_{max} with increasing M_w which we attribute to changes of the average polymer chain orientation as will be discussed below. We note that the deviation of **5** from this trend is related to its much larger polydispersity as compared to **4** and **6**. The influence of polydispersity will deserve further attention in our future studies.

The dispersions of n_{TE} of polymers **4**, **6**, and **8** are shown with solid lines in Figure 2. They are evaluated from reflectometry measurements. Similar to the intrinsic absorption coefficient, n_{TE} increases for higher molecular weight MEH-PPVs.

MEH-PPV waveguides with typical thicknesses ranging from 400 to 800 nm were studied by the prism coupling technique[7,39] to determine the refractive index *n* at several laser wavelengths between 633 and 1100 nm. The dispersions of n_{TE} and n_{TM} are shown with symbols in Figure 2 for the MEH-PPVs **4**, **6**, and **8**. Again, we observe a very pronounced influence of M_w on the refractive index and its birefringence $\Delta n = n_{TE} - n_{TM}$. The results of prism coupling and reflectometry agree very well, which indicates that n_{TE} is not depending significantly on the film thickness, at least for $d = 70$ and 800 nm. The thickness dependence of n_{TE} and n_{TM} will be presented below.

Figure 3 shows n_{TE} and n_{TM} at $\lambda = 633$ nm as a function of M_w for all polymers studied. At high molecular weights ($M_w >$ 400 kg/mol) the birefringence is very large and nearly independent of M_w. The values of n_{TE}, and n_{TM} in this region are in good agreement with those reported recently.[10−12] With the decrease of the molecular weight the birefringence is significantly reduced, and at $M_w < 15$ kg/mol we observe a nearly complete loss of birefringence with a remaining $\Delta n < 0.005$. We emphasize that although MEH-PPVs were synthesized in different laboratories via different routes, the results displayed

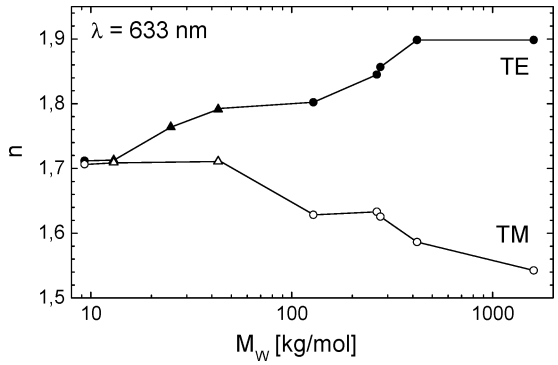

Figure 3. Molecular weight dependence of the refractive index of thin films of MEH-PPVs **1**−**8** measured by prism coupling at 633 nm using transverse electric (TE) and transverse magnetic (TM) polarizations. n_{TE} of **9** is measured by reflectometry, and n_{TM} of **9** is extrapolated from ref 12. Symbols refer to synthetic routes: Horner (triangles), Gilch (circles).

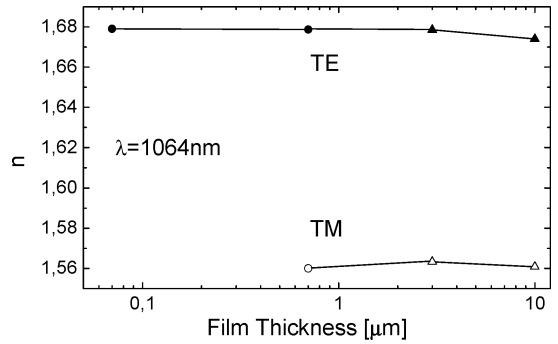

Figure 4. Semilogarithmic plot of in plane (n_{TE}, full symbols) and out-of-plane (n_{TM}, open symbols) refractive indices of thin films of MEH-PPV **7** measured at 1064 nm as a function of the film thickness. The circles correspond to films made with spin-coating and the triangles to films made with doctor blading.

in Figure 3 show good reproducibility and a nearly continuous dependence of the birefringence on the molecular weight. This is a clear indication for the dominant influence of M_w on the chain orientation effects, whereas the synthetic pathways have minor impact here.

Taking into account that the values of n_{TE} and n_{TM} shown in Figure 3 were measured in films with typical thicknesses $d \approx$ 400−800 nm, it may look tempting to explain the increase of the in-plane orientation with M_w by confinement effects. The average contour length is defined as the length of the repeat unit multiplied by the average number of units as derived from M_n. Indeed, the low molecular weight MEH-PPVs **1** and **2** have a contour length of about 10−20 nm, i.e., much smaller than *d*, while that of the high-M_w samples **7**−**9** is larger than 250 nm, i.e., on the order of the film thickness. To explore this possibility of chain confinement effects, we studied the thickness dependence of the birefringence of the high molecular weight MEH-PPV **7**. The films were prepared by means of spin-coating (70 nm $< d <$ 1 μm) and doctor-blading ($d = 3$ μm and 10 μm). Figure 4 shows n_{TE} and n_{TM} at $\lambda = 1064$ nm as a function of the film thickness. We like to elucidate the following points. First of all, we had to use the transmission−reflection spectroscopy to study the thinnest film ($d = 70$ nm) as it was too thin to support waveguide modes. We were able to measure only n_{TE} of this film because our reflectometry method does not yield n_{TM}. All other films were studied with waveguide prism coupling. Figure 4 shows that the films made by spin-coating and doctor-blading have very similar refractive indices. Therefore, their morphology must be similar. This observation indicates that the preferred alignment of the polymer chains

should be related to the intrinsic properties of the MEH-PPV and to substrate−polymer interactions and not to the particular film preparation method, at least for this particular range of film thicknesses and molecular weights. Furthermore, the birefringence ($n_{TE} - n_{TM}$) does not decrease significantly with the increase of d up to a film thickness of 10 μm. This observation shows that chain confinement effects at reduced film thicknesses alone are not appropriate to explain the increased alignment of the high molecular weight MEH-PPV samples for the following reason: The average contour length of **7**, estimated from M_n, is only ∼260 nm and significantly smaller than the thickness range of 3−10 μm where we still observe nearly the same Δn as for ultrathin films.

It is interesting to compare our results on the thickness dependence of Δn with reports of other groups. Earlier studies have shown that the birefringence of thin polymer films may depend on the film thickness, as for example in the case of polystyrene[19] or polythiophene.[22] Other polymers, however, e.g. polyimides,[21,43] do not show a thickness dependence of Δn for films with thicknesses starting from 1 μm and up to a critical thickness in the order of several micrometers. The observed absence of a significant thickness dependence of Δn up to $d =$ 10 μm in the high molecular weight MEH-PPV films is similar to the reported behavior of polyimides.[21,43] Therefore, we expect that a similar mechanism, i.e., the liquid crystalline behavior of the MEH-PPV chains owing to their limited chain flexibility, is causing the alignment of the chain segments parallel to the layer plane as observed in spin-cast thin films of several other polymers with significant chain rigidity.[16,43]

Refractive index and absorption coefficient α_{max} are correlated to each other. Both quantities can show significant anisotropy in thin films. The electronic $\pi-\pi^*$ transition at λ_{max} and the electric polarizability, which is related to n, are both highly polarized and have their main components in the chain direction of PPV.[44] Consequently, α_{max} and n are largest if the electric field **E** of incident light is parallel to the chain direction. If the PPV chains become increasingly aligned parallel to the substrate plane, it is evident that α_{max}, which is measured at **E** parallel to the film plane, and n_{TE} will increase, and correspondingly, n_{TM} will decrease. Our experimental results show this correlated dependence of n_{TE}, n_{TM}, and α_{max} on M_w quite well. This behavior strongly indicates that thin films of MEH-PPVs with larger M_w have an increasing amount of PPV chain segments aligned parallel to the substrate plane. This conclusion is further supported by the results of FTIR spectroscopy presented in the next chapter and is in line with the similar results reported for a polydiacetylene[20] or a polyimide.[21]

FTIR Spectroscopy. We used Fourier transform infrared (FTIR) spectroscopy to study the average chain orientation in thin films of MEH-PPV with typical thickness of 70 nm. Infrared spectroscopy with polarized light is a well-known technique for determining molecular orientation.[42,45] As the transition dipole moment vector of a vibration mode is oriented at a specific angle φ relative to the chain axis, the IR spectra can be used to obtain information on the chain orientation by comparing the relative strength of vibration bands with different φ.[42,45,46] We measured IR spectra of thin films of **4**, **6**, and **8** in two configurations: transmission and grazing incidence reflection. Transmission spectra at perpendicular incidence have the electrical field vector oriented parallel to the plane of film, $\mathbf{E}_{||}$, and reflection spectra at grazing incidence result in the perpendicular orientation, $\mathbf{E}_{\perp}$. The FTIR spectra of thin films of **4** and **8** are displayed in Figure 5. The following IR bands can be used to indicate the chain orientation because their

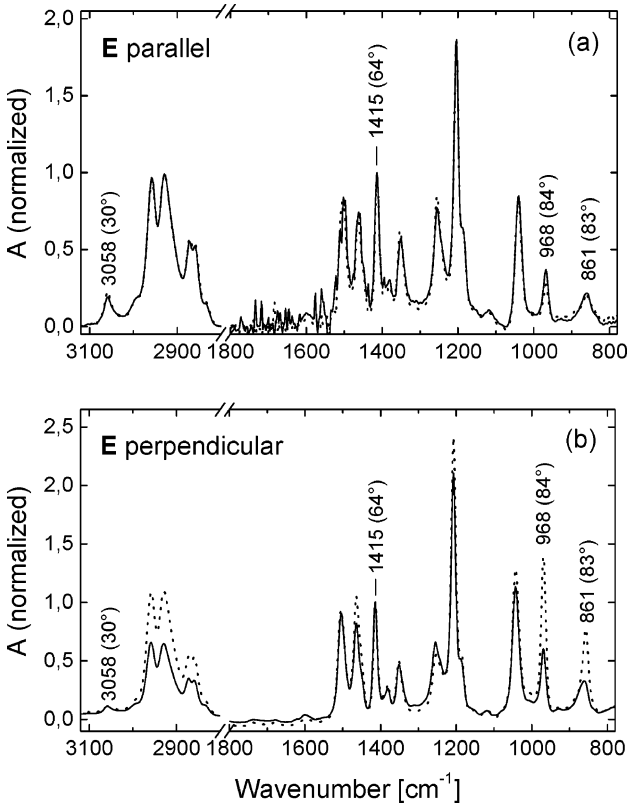

Figure 5. FTIR spectra of MEH-PPVs **4** (solid line) and **8** (dashed line). Absorbance A is normalized with respect to the band at 1415 cm^{-1}. Wavenumbers and angles φ are shown for selected bands only. (a) Transmission spectroscopy at perpendicular incidence with **E** parallel to the layer plane. (b) Reflection spectroscopy at grazing incidence with **E** perpendicular to the layer plane.

assignment to molecular vibrations and angles φ are known from earlier work:[3,46,47] 861 cm^{-1} (out-of-plane phenyl CH wag, $\varphi = 83°$); 968 cm^{-1} (*trans*-vinylene CH wag, $\varphi = 84°$); 1415 cm^{-1} (semicircular phenyl stretch, $\varphi = 64°$); 3058 cm^{-1} (*trans*-vinylene C−H stretch, $\varphi = 30°$). As the spectra were measured from films with slightly different thicknesses, we used the band at 1415 cm^{-1} for normalization of the spectra. The transition dipole moment vector of the vibration mode of this band is oriented at the angle $\varphi = 64°$, i.e., neither parallel nor perpendicular to the chain axis, making this band particularly suitable for normalization when a study of the chain orientation is considered. We emphasize, however, that this normalization was done for better presentation of the experimental data only, and it does not influence any of the conclusions derived below. The relative intensities of the bands with $\varphi = 83°$ and $\varphi = 84°$ are small for $\mathbf{E}_{||}$ (Figure 5a) and much larger for $\mathbf{E}_{\perp}$ (Figure 5b). This is already clear evidence for a preferred orientation of the polymer chains in the plane of the film. The same conclusion can be derived from the behavior of the band at 3058 cm^{-1} ($\varphi = 30°$), which is stronger for $\mathbf{E}_{||}$ as compared to $\mathbf{E}_{\perp}$. The degree of chain orientation is strongly dependent on the M_w of the MEH-PPVs, which is especially evident if we look at the bands at 861 cm^{-1} ($\varphi = 83°$) and 968 cm^{-1} ($\varphi = 84°$) for $\mathbf{E}_{\perp}$ in Figure 5b. These bands become stronger with growing M_w from **4** to **6** (not shown) and **8,** which indicates an increasing alignment of chains parallel to the film plane. To describe this orientation effect more quantitatively (and independent of any normalization of the spectra), we use the ratio R of the absorbances A of the bands at 968 cm^{-1} ($\varphi = 84°$) and 3058 cm^{-1} ($\varphi = 30°$), which we define as $R = A_{968}/A_{3058}$. Let us consider first the case when the electrical field vector **E** of the

Table 2. Comparison of the Ratio $R = A_{968}/A_{3058}$ of the IR Absorbances of the Bands at 968 cm^{-1} ($\varphi = 84°$) and 3058 cm^{-1} ($\varphi = 30°$) Measured for Incident Electric Field Perpendicular ($E_\perp$) and Parallel ($E_\parallel$) to the Film Plane, Respectively

polymer	M_w [kg/mol]	R at $E_\perp$	R at $E_\parallel$
4	40.3	8	1.8
6	265	14	1.5
8	420	22	1.0

incident light is perpendicular to the film plane. Then if the polymer chains are oriented perfectly parallel to the film plane, the transition dipole moment vector of the vibration mode of the band at 968 cm^{-1} ($\varphi = 84°$) will be almost parallel to **E** and the absorbance A_{968} will be very large. In contrast, the transition dipole moment vector of the vibration mode at 3058 cm^{-1} ($\varphi = 30°$) will be more perpendicular to **E** with the consequence that A_{3058} will be very small. In this way, we expect that the ratio $R = A_{968}/A_{3058}$ should be large if the polymer chains are parallel to the film plane. In the second case of a randomly oriented sample, the absorbance at 968 cm^{-1} will decrease because of reduced spatial overlap between the transition dipole and **E**, and consequently, the absorbance at 3058 cm^{-1} will increase. In this way, the ratio R should be significantly smaller for the randomly oriented chains as compared to chains oriented parallel to the substrate. Similar considerations can be made for the case that the electric field of the incident light is parallel to the film surface. One can show that the ratio R should be bigger for the randomly oriented chains as compared to chains oriented parallel to the substrate.

The values of R evaluated for polymers **4**, **6**, and **8** are shown in Table 2. It can be seen that for $\mathbf{E}_\perp$ R increases with M_w, whereas R decreases with M_w in the case of $\mathbf{E}_\parallel$. This is clear evidence that the polymer chain segments become aligned more parallel to the layer plane at higher molecular weights.

An additional question is the orientation of the planes of the aromatic rings and the *trans*-vinylene groups with respect to the substrate plane. An earlier X-ray diffraction study of solution-cast MEH-PPV films has shown that both the PPV backbones and the planes defined by the benzene rings within the PPV backbones are oriented preferably parallel to the film plane.[48] Our FTIR spectra of high molecular weight MEH-PPV spin-cast films reveal a similar orientation behavior: The bands at 861 and 968 cm^{-1} have moments mainly perpendicular to the planes of the aromatic rings and the *trans*-vinylene groups, respectively.[46] These specific bands appear strongest at $\mathbf{E}_\perp$, which is clear evidence for the preferred orientation of the aromatic rings parallel to the layer plane.

Finally, the FTIR data could be used for assessment of a possible photooxidation of the MEH-PPV samples. It is well-known that the photooxidation of PPVs leads to the appearance of a C═O stretching mode in the spectral region around 1700 cm^{-1}.[49] As can be seen in Figure 5, no major absorption is observed in this region, which indicates that our results were not influenced by photodegradation of the MEH-PPV films.

Waveguide Propagation Loss. The waveguide propagation loss is an important parameter which serves as quantitative measure for the optical quality of thin films. High-quality slab waveguides for applications in optoelectronics should have a smallest possible total waveguide propagation loss coefficient α_{gw}, which is defined as the sum of the intrinsic absorption coefficient α and the scattering losses. Because both parameters may strongly depend on the film morphology, we have measured α_{gw} of slab waveguides made from the different molecular weight MEH-PPVs **1**−**8** using the following procedure: A propagation mode in the waveguide was excited by prism coupling. The scattered light of the waveguide mode was imaged on a diode array (see the Experimental Section). Typical dependencies of the scattered light intensity as a function of the distance from the prism for TE_0 mode at the wavelength 1064 nm are shown in Figure 6, which indicates that the decrease of scattered light intensity with propagation distance is very small in the case of **1** and significantly larger for **7**. As the intensity of the light scattered out of the film is proportional to the guided wave intensity, the waveguide loss coefficient α_{gw} is determined by the slope of the linear fit of the data as shown in the example of Figure 6. The data of $\alpha_{gw}(TE_0)$ and $\alpha_{gw}(TM_0)$ at the wavelength 1064 nm are presented in Table 1 for all MEH-PPVs studied. Waveguides prepared from low molecular weight MEH-PPVs **1**−**4** have unprecedented low attenuation losses $\alpha_{gw}(TE_0) < 1$ dB/cm, whereas the higher molecular weight samples **5**−**8** have significantly larger $\alpha_{gw}(TE_0)$ which increase strongly with M_w. Interestingly, Table 1 shows that *all* MEH-PPVs studied at TM polarization have nearly identical data of $\alpha_{gw}(TM_0)$ in the range 0.5−1.0 dB/cm.

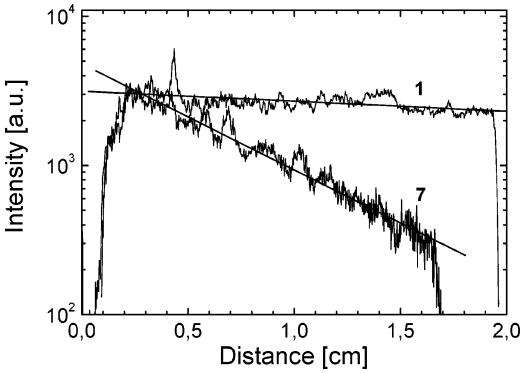

Figure 6. Intensity of the light scattered from TE_0 modes of waveguides of MEH-PPVs **1** and **7** vs distance from the coupling prism at $\lambda = 1064$ nm. The lines represent the loss coefficients α_{gw}, as presented in Table 1.

As the intrinsic absorption of MEH-PPV waveguides is negligibly small at 1064 nm, the measured loss coefficients α_{gw} are caused by scattering losses only. Light scattering can arise from surface roughness and from scattering within the film. The average surface roughness of the MEH-PPV waveguides, as measured with surface profilometry, was rather low (on the order of 1−2 nm[6]) and did not show any significant dependence on M_w. Therefore, we have to discuss our data in terms of the morphology of the films.

Whereas films of the low-M_w (Horner route) MEH-PPVs were reported to be amorphous,[13] films of high-M_w (Gilch route) MEH-PPVs may show a nematic-like texture.[50,51] It was also reported that gel formation and aggregation phenomena can occur already in solutions of high-M_w MEH-PPVs.[52−54] These aggregates can be preserved through the casting process and are observed in the films.[48,53,55] We note a rather different solubility of the various MEH-PPVs. Low-M_w MEH-PPVs **1**−**4** were easily dissolved in concentrations by weight up to 7%, and these solutions were filtered easily with 0.5 μm micropore filters. However, we were not able to dissolve the higher molecular weight polymers **5**−**9** in high concentrations due to problems related to their high viscosity and gelation problems. For example, solutions of **9** show gelation problems already at concentrations > 1 wt %. Moreover, solutions of **5**−**9** could not be filtered with the 0.5 μm micropore filter. Therefore, we had to use the next larger pore size of 1 μm. It may be that the probability for the appearance of aggregates in solution is larger for the high-M_w samples of MEH-PPV.

We conclude that the morphology of the MEH-PPV films is mainly responsible for the observed waveguide losses presented in Table 1. The major observations are (i) $\alpha_{gw}(TE_0)$ increases strongly with M_w, and (ii) $\alpha_{gw}(TM_0)$ is small and independent of M_w. We interpret these effects by light scattering which is caused by local changes of the refractive index at the boundary regions between intrinsically ordered regions which we call here "aggregation domains" for simplicity. Such aggregates were reported for solution cast films of MEH-PPV.[48,50,51,55] But a discussion of their detailed structure is beyond our scope. We assume that the chain segments within these domains are oriented preferably parallel to each other and show an increased tendency to align parallel to the layer plane with increasing M_w. This hypothesis is in line with our results of FTIR and optical spectroscopy presented above and, furthermore, with the observation of nematic-like textures and nanodomains in thin films of high-M_w MEH-PPV.[48,50,51,55] Consequently, the propagation losses α_{gw} should depend on the polarization of the waveguide mode in the following way:

TE waveguide modes have the electric field vector **E** oriented in the film plane. The local refractive index *n* will change strongly, if the wave propagates through the boundary region between differently oriented domains. The local component of the anisotropic *n* of a domain will be largest (smallest) for **E** parallel (perpendicular) to the directions of the PPV backbones. Consequently, the loss coefficient $\alpha_{gw}(TE_0)$ will depend strongly on the relative amount and the size of these aggregation domains which both may grow with increasing M_w. This hypothesis explains the strong increase of $\alpha_{gw}(TE_0)$ with M_w, as shown in Table 1.

TM polarization, on the other hand, causes an orientation of **E** mainly perpendicular to the PPV chain directions in the domains. Therefore, the local changes of the refractive index at the boundary regions between domains are rather small and independent of the different lateral orientations of the domains and the polymer backbones. This model explains why we observe nearly the same and very small loss coefficients $\alpha_{gw}(TM_0)$ for all MEH-PPVs independent of their M_w.

Conclusion

We have shown that the orientation of the polymer chain segments depends significantly on the molecular weight, especially in the range $M_w < 400$ kg/mol. Thin films of *high* molecular weight MEH-PPV have most chain segments oriented parallel to the layer plane—in contrast to *low* molecular weight samples which have nearly random orientation of the chain segments. It is very likely that other conjugated polymers with similar rigid backbones will also show such orientation phenomena. In this sense the control of the molecular weight may be a key factor for good reproducibility of the morphology, optoelectronic properties, and optical constants of thin films of conjugated polymers.

From the application point of view it is important to emphasize that the appropriate choice of the molecular weight of MEH-PPV enables fine-tuning of the refractive index of thin films and optical waveguides. Furthermore, our results are useful for the selection procedure of the most appropriate type of MEH-PPV for specific applications in optoelectronics, for example: OLEDs should perform better with *high*-M_w polymers because the enhanced in-plane alignment may facilitate the intermolecular charge transport and the light emission perpendicular to the layer plane,[2,3,29,30] which is also of concern for transistors.[24−27] On the other hand, waveguide applications (such as plastic lasers[1,23] and linear and nonlinear integrated optical devices[7,8,15,56]) require ultimately low waveguide propagation losses that can be achieved preferably by means of *low*-M_w polymers.

Acknowledgment. We thank Dr. H. Becker (Covion) for the gift of MEH-PPV (polymer **9**) and G. Herrmann and W. Scholdei for their help with film preparation and optical spectroscopy, respectively. Financial support was given in parts by the European Community (Marie Curie Fellowship to K.K.), Deutscher Akademischer Austauschdienst (PhD stipend to A.B. and R.M.C.), Alexander von Humboldt Foundation (T.A.), Bundesministerium für Bildung und Forschung, and Fonds der Chemischen Industrie (C.B.).

References and Notes

(1) McGehee, M. D.; Heeger, A. J. *Adv. Mater.* **2000**, *12*, 1655.
(2) Friend, R. H.; Gymer, R. W.; Holmes, A. B.; Burroughes, J. H.; Marks, R. N.; Taliani, C.; Bradley, D. D. C.; Dos Santos, D. A.; Bredas, J. L.; Lögdlund, M.; Salaneck, W. R. *Nature (London)* **1999**, *397*, 121.
(3) Scott, J. C.; Kaufman, J. H.; Brock, P. J.; DiPietro, R.; Salem, J.; Goitia, J. A. *J. Appl. Phys.* **1996**, *79*, 2745.
(4) Schwartz, B. J. *Annu. Rev. Phys. Chem.* **2003**, *54*, 141.
(5) Bubeck, C.; Ueberhofen, K.; Ziegler, J.; Fitrilawati, F.; Baier, U.; Eichner, H.; Former, C.; Müllen, K.; Pfeiffer, S.; Tillmann, H.; Hörhold, H.-H. *Nonlinear Opt.* **2000**, *25*, 93.
(6) Fitrilawati, F.; Tjia, M. O.; Pfeiffer, S.; Hörhold, H.-H.; Deutesfeld, A.; Eichner, H.; Bubeck, C. *Opt. Mater.* **2002**, *21*, 511.
(7) Koynov, K.; Goutev, N.; Fitrilawati, F.; Bahtiar, A.; Best, A.; Bubeck, C.; Hörhold, H.-H. *J. Opt. Soc. Am. B* **2002**, *19*, 895.
(8) Bader, M. A.; Marowsky, G.; Bahtiar, A.; Koynov, K.; Bubeck, C.; Tillmann, H.; Hörhold, H.-H.; Pereira, S. *J. Opt. Soc. Am. B* **2002**, *19*, 2250.
(9) McBranch, D.; Campbell, I. H.; Smith, D. L.; Ferraris, J. P. *Appl. Phys. Lett.* **1995**, *66*, 1175.
(10) Boudrioua, A.; Hobson, P. A.; Matterson, B.; Samuel, I. D. W.; Barnes, W. L. *Synth. Met.* **2000**, *111−112*, 545.
(11) Wasey, J. A. E.; Safonov, A.; Samuel, I. D. W.; Barnes, W. L. *Phys. Rev. B* **2001**, *64*, 205201.
(12) Tammer, M.; Monkman, A. P. *Adv. Mater.* **2002**, *14*, 210. According to the private communication of A. P. Monkman, MEH-PPV used in this work had $M_w = 1.6 \times 10^6$ g/mol as specified by the supplier.
(13) Kranzelbinder, G.; Toussaere, E.; Zyss, J.; Pogantsch, A.; List, E. W. J.; Tillmann, H.; Hörhold, H.-H. *Appl. Phys. Lett.* **2002**, *80*, 716.
(14) Bahtiar, A.; Koynov, K.; Bubeck, C.; Bader, M. A.; Wachsmuth, U.; Marowsky, G. In *OSA Trends in Optics and Photonics (TOPS) Vol. 80, Nonlinear Guided Waves and Their Applications*; OSA Technical Digest, Postconference Edition; Optical Society of America: Washington, DC, 2002; p NLMD58-1.
(15) Koynov, K.; Bahtiar, A.; Ahn, T.; Bubeck, C.; Hörhold, H.-H. *Appl. Phys. Lett.* **2004**, *84*, 3792.
(16) Losurdo, M.; Giangregorio, M. M.; Capezzuto, P.; Bruno, G.; Babudri, F.; Colangiuli, D.; Farinola, G. M.; Naso, F. *Macromolecules* **2003**, *36*, 4492.
(17) Rau, I.; Armatys, P.; Chollet, P.; Kajzar, F.; Zamboni, R. *Mol. Cryst. Liq. Cryst.* **2006**, *446*, 23.
(18) Campoy-Quiles, M.; Etchegoin, P. G.; Bradley, D. D. C. *Phys. Rev. B* **2005** *72*, 045209.
(19) Prest, W. M.; Luca, D. J. *J. Appl. Phys.* **1980**, *51*, 5170.
(20) Grando, D.; Banfi, G. P.; Fortusini, D.; Ricceri, R.; Sottini, S. *Synth. Met.* **2003**, *139*, 863.
(21) Li, F.; Kim, K.-H.; Savitski, E. P.; Chen, J.-C.; Harris, F. W.; Cheng, S. Z. D. *Polymer* **1997**, *38*, 3223.
(22) Zhokhavets, V.; Gobsch, G.; Hoppe, H.; Sariciftci, N. S. *Thin Solid Films* **2004**, *69*, 451.
(23) Holzer, W.; Penzkofer, A.; Tillmann, H.; Hörhold, H.-H. *Synth. Met.* **2004**, *140*, 155.
(24) Shaked, S.; Tal, S.; Roichman, Y.; Razin, A.; Xiao, S.; Eichen, Y.; Tessler, N. *Adv. Mater.* **2003**, *15*, 913.
(25) Kline, R.; McGehee, M.; Kadnikova, E.; Liu, J.; Frechet, J. *Adv. Mater.* **2003**, *15*, 1519.
(26) Zen, A.; Pflaum, J.; Hirschmann, S.; Zhuang, W.; Jaiser, F.; Asawapirom, U.; Rabe, J.; Scherf, U.; Neher, D. *Adv. Funct. Mater.* **2004**, *14*, 757.
(27) Kline, R.; McGehee, M.; Kadnikova, E.; Liu, J.; Frechet, J.; Toney, M. *Macromolecules* **2005**, *38*, 3312.
(28) Zen, A.; Saphiannikova, M.; Neher, D.; Grenzer, J.; Grigorian, S.; Pietsch, U.; Asawapirom, U.; Janietz, S.; Scherf, U.; Lieberwirth, I.; Wegner, G. *Macromolecules* **2006**, *39*, 2162.

(29) Donley, C.; Zaumseil, J.; Andreasen, J.; Nielsen, M.; Sirringhaus, H.; Friend, R.; Kim, J. *J. Am. Chem. Soc.* **2005**, *127*, 12890.
(30) Banach, M. J.; Friend, R. H.; Sirringhaus, H. *Macromolecules* **2003**, *36*, 2838.
(31) Knaapila, M.; Lyons, B. P.; Hase, T. P. A.; Pearson, C.; Petty, M. C.; Bouchenoire, L.; Thompson, P.; Serimaa, R.; Torkkeli, M.; Monkman, A. P. *Adv. Funct. Mater.* **2005**, *15*, 1517.
(32) Knaapila, M.; Stepanyan, R.; Lyons, B. P.; Torkkeli, M.; Hase, T. P. A.; Serimaa, R.; Guntner, R.; Seeck, O. H.; Scherf, U.; Monkman, A. P. *Macromolecules* **2005**, *38*, 2744.
(33) Gilch, H. G.; Wheelwright, W. L. *J. Polym. Sci., Part A-1: Polym. Chem.* **1966,** *4*, 1337.
(34) Wudl, F.; Sradanov, G. US Pat. 5189136.
(35) Pfeiffer, S.; Hörhold, H.-H. *Macromol. Chem. Phys.* **1999**, *200*, 1870.
(36) Ahn, T.; Ko, S. W.; Lee, J.; Shim, H. K. *Macromolecules* **2002**, *35*, 3495.
(37) Lee, J. W.; Wang, C. S. *Polymer* **1994**, 3673.
(38) Mathy, A.; Ueberhofen, K.; Schenk, R.; Gregorius, H.; Garay, R.; Müllen, K.; Bubeck, C. *Phys. Rev. B* **1996**, *53*, 4367.
(39) Ulrich, R.; Torge, R. *Appl. Opt.* **1973**, *12*, 2901.
(40) Mathy, A.; Simmrock, H.-U.; Bubeck, C. *J. Phys. D: Appl. Phys.* **1991**, *24*, 1003.
(41) Greenler, R. G. *J. Chem. Phys.* **1966**, *44*, 310.
(42) Bubeck, C.; Holtkamp, D. *Adv. Mater.* **1991**, *3*, 32.
(43) Boese, D.; Lee, H.; Yoon, D. Y.; Swalen, J. D.; Rabolt, J. F. *J. Polym. Sci., Part B: Polym. Phys.* **1992**, *30*, 1321.
(44) Hagler, T. W.; Pakbaz, K.; Moulton, J.; Wudl, F.; Smith, P.; Heeger, A. *J. Polym. Commun.* **1991**, *32*, 339.
(45) Michl, J.; Thulstrup, E. W. *Spectroscopy with Polarized Light*; VCH Publishers: New York, 1995.
(46) Bradley, D. D. C.; Friend, R. H.; Lindenberger, H.; Roth, S. *Polymer* **1986**, *27*, 1709.
(47) Tian, B.; Zerbi, G.; Müllen, K. *J. Chem. Phys.* **1991**, *95*, 3198.
(48) Yang, C. Y.; Hide, F.; Diaz-Garcia, M. A.; Heeger, A. J.; Cao, Y. *Polymer* **1998**, *39*, 2299.
(49) Rothberg, L. J.; Yan, M.; Papadimitrakopoulos, F.; Galvin, M. E.; Kwock, E. W.; Miller, T. M. *Synth. Met.* **1996**, *80*, 41.
(50) Chen, S.-H.; Su, A.-C.; Huang, Y.-F.; Su, C.-H.; Peng, G.-Y.; Chen, S.-A. *Macromolecules* **2002**, *35*, 4229.
(51) Chen, S. H.; Su, A. C.; Chou, H. L.; Peng, K. Y.; Chen, S. A. *Macromolecules* **2004**, *37*, 167.
(52) Nguyen, T.-Q.; Doan, V.; Schwartz, B. J. *J. Chem. Phys.* **1999**, *110*, 4068.
(53) Nguyen, T.-Q.; Martini, I. B.; Liu, J.; Schwartz, B. J. *J. Phys. Chem. B* **2000**, *104*, 237.
(54) Ou-Yang, W.-C.; Chang, C.-S.; Chen, H.-L.; Tsao, C.-S.; Peng, K.-Y.; Chen, S.-A.; Han, C. C. *Phys. Rev. E* **2005**, *72*, 031802.
(55) Jeng, U.; Hsu, C.-H.; Sheu, H.-S.; Lee, H.-Y.; Inigo, A. R.; Chiu, H. C.; Fann, W. S.; Chen, S. H.; Su, A. C.; Lin, T.-L.; Peng, K. Y.; Chen, S. A. *Macromolecules* **2005**, *38*, 6566.
(56) Stegeman, G. I. *Proc. SPIE* **1993**, *1852*, 75.

MA0611164